VOL. 103 NO. GT9. SEPT. 1977

JOURNAL OF THE GEOTECHNICAL ENGINEERING DIVISION

PROCEEDINGS OF
THE AMERICAN SOCIETY
OF CIVIL ENGINEERS

AMERICAN SOCIETY OF CIVIL ENGINEERS
FOUNDED 1852

VOL. 103 NO. GT9. SEPT. 1977

JOURNAL OF THE GEOTECHNICAL ENGINEERING DIVISION

PROCEEDINGS OF THE AMERICAN SOCIETY OF CIVIL ENGINEERS

CONTENTS

TECHNICAL NOTES

Proc. Paper 13242

→

This Journal is published monthly by the American Society of Civil Engineers. Publications office is at 345 East 47th Street, New York, N.Y. 10017. Address all ASCE correspondence to the Editorial and General Offices at 345 East 47th Street, New York, N.Y. 10017. Allow six weeks for change of address to become effective. Subscription price to members is $12.00. Nonmember subscriptions available; prices obtainable on request. Second-class postage paid at New York, N.Y. and at additional mailing offices. GT, HY.

DISCUSSION

Proc. Paper 13164

INFORMATION RETRIEVAL

The key words, abstract, and reference "cards" for each article in this Journal represent part of the ASCE participation in the EJC information retrieval plan. The retrieval data are placed herein so that each can be cut out, placed on a 3 × 5 card and given an accession number for the user's file. The accession number is then entered on key word cards so that the user can subsequently match key words to choose the articles he wishes. Details of this program were given in an August, 1962 article in CIVIL ENGINEERING, reprints of which are available on request to ASCE headquarters.

[a]Discussion period closed for this paper. Any other discussion received during this discussion period will be published in subsequent Journals.

13223 UPLIFT RESISTANCE OF COHESIVE SOILS

KEY WORDS: Anchors; Clays; **Cohesive soils;** Dimensional analysis; Finite elements; **Models; Pull-out tests; Uplift resistance**

ABSTRACT: Effects of vertical uplift forces on circular anchors in purely cohesive soils are considered. Model tests indicate a general type of ultimate uplift failure in shallow anchors, occurring by yielding above and below the anchor due to shear and tensile stresses and cracking in the soil. Existing shallow anchor theories, although in substantial agreement with one another, overestimate actual ultimate uplift resistance since they do not take into account tensile stresses and cracking. Model tests indicate a local type of failure in deep anchors and confirm existing deep anchor theories that take account of soil compressibility. Dimensional analysis indicates that caution must be exercised when interpreting model uplift test results in terms of the prototype, particularly when the prototype soil has low shear strength. A finite element program has been developed to estimate, within limitations, the magnitude and direction of stresses occurring in each element of the mesh at any stage of uplift resistance.

REFERENCE: Davie, John R., and Sutherland, Hugh B., "Uplift Resistance of Cohesive Soils," *Journal of the Geotechnical Engineering Division,* ASCE, Vol. 103, No. GT9, **Proc. Paper 13223**, September, 1977, pp. 935-952

13214 ENGINEERING OF GROUT CURTAINS TO STANDARDS

KEY WORDS: **Dam construction; Dam design; Dams;** Dams (arch); Dams (concrete); Dams (gravity); Dams (rockfill); Drainage; Field tests; Foreign engineering; **Foundations; Grouting; Permeability; Pore water pressure;** Seepage; **Standards;** Tests

ABSTRACT: The desirable permeabilities of curtains vary for different types of dams and conditions. The paper examines these issues and for them suggests standards of permeability expressed in lugeon units. To engineer curtains to desired standards, the split spacing or closure method is used, and closure is preserved until the target standards are reached. This procedure is applied to hole spacing and, separately, to hole depth. The upper stages of curtains can be constructed to tighter permeabilities than lower stages. At earth core dams, the curtain permeability should ideally produce pore pressures immediately above the foundation slightly in excess of pressures in foundation joints. The curtain's position affects the ideal permeability. At concrete dams, the curtain permeability should relate to the ability of the drainage system to discharge seepage.

REFERENCE: Houlsby, Adam Clive, "Engineering of Grout Curtains to Standards," *Journal of the Geotechnical Engineering Division,* ASCE, Vol. 103, No. GT9, **Proc. Paper 13214**, September, 1977, pp. 953-970

13221 THREE-DIMENSIONAL SLOPE STABILITY ANALYSIS

KEY WORDS: **Equilibrium methods;** Landslides; **Limit design method;** Mathematical models; Slope protection; **Slope stability; Stability analysis; Three-dimensional**

ABSTRACT: Existing limit-equilibrium stability analysis methods are two-dimensional; a few methods for correcting or extending a two-dimensional analysis have been proposed. Presented in this paper is a general method for three-dimensional limit-equilibrium stability analysis. Limiting cases are considered in order to study preliminary implications of three-dimensional stability analyses. The method lends itself to both hand calculation and computer application. Method can also be used together with finite element analysis which should make it possible to set up a fairly realistic model for soil and slope behavior.

REFERENCE: Hovland, H. John, "Three-Dimensional Slope Stability Analysis Method," *Journal of the Geotechnical Engineering Division,* ASCE, Vol. 103, No. GT9, **Proc. Paper 13221**, September, 1977, pp. 971-986 and foundation conditions. Typical values are shown in Fig. 1 for standards of watertightness.

Methods are detailed in the paper for obtaining specified standards of permeability. These methods are suitable for use by very experienced personnel.

Acknowledgment

The writer wishes to acknowledge the permission given by the Water Resources Commission of New South Wales to use information from projects.

Appendix.—References

1. Burwell, E. B., "Cement and Clay Grouting of Foundations: Practice of the Corps of Engineers," *Journal of the Soil Mechanics and Foundations Division*, ASCE, Vol. 84, No. SM1, Proc. Paper 1551, Feb., 1958, pp. 1551-15-1551-22.
2. *Grouting Manual*, Water Resources Commission, New South Wales, Australia, 1973.
3. Houlsby, A. C., discussion of "Rock Fracture Spacings, Openings and Porosities," by David J. Snow, *Journal of the Soil Mechanics and Foundations Division*, ASCE, Vol. 95, No. SM1, Proc. Paper 6324, Jan., 1969, pp. 416-417.
4. Houlsby, A. C., "Routine Interpretation of the Lugeon Water Test," *Quarterly Journal of Engineering Geology*, The Geological Society, London, England, Vol. 9, 1976, pp. 303-313.
5. John, K. W., "Graphical Stability Analysis of Slopes in Jointed Rock," *Journal of the Soil Mechanics and Foundations Division*, ASCE, Vol. 94, No. SM2, Proc. Paper 5865, Mar., 1968, pp. 497-526.
6. Lugeon, M., *Barrages et Geologie*, Lausanne, Paris, France, 1933.
7. Morgenstern, N. R., and Vaughan, P. R., "Some Observations on Allowable Grouting Pressures," Symposium on Grouts and Drilling Muds in Engineering Practice, Butterworths, London, England, 1963, pp. 36-42.
8. Singhota, J. S., "Grout Hole Orientation—Mathematical Solution," *Journal of the Soil Mechanics and Foundations Division*, ASCE, Vol. 95, No. SM4, Proc. Paper 6660, July, 1969, pp. 995-1006.

JOURNAL OF THE GEOTECHNICAL ENGINEERING DIVISION

Three-Dimensional Slope Stability Analysis Method

By H. John Hovland,[1] M. ASCE

Introduction

Many kinds of problems in geotechnical engineering require limit-equilibrium stability analysis. Any situation in which the earth materials are stressed to the point that slip occurs and in which the body of materials that are slipping can be described can be analyzed with a limit-equilibrium type of analysis. By the more usual, but restricted, definition, limit-equilibrium stability analysis refers to slope stability analysis.

The geotechnical literature describes numerous landslide case histories (1). These case histories usually deal with the larger landslides; analysis, exploration, testing, post-failure analysis, and corrective measures are described. Because of the many assumptions necessary in stability analyses, case histories are, of course, of fundamental importance.

Past research has concentrated on refining two-dimensional analysis techniques. Rather extensive comparisons of various two-dimensional methods have been made (10,11). These show that, for two-dimensional analyses to be generally accurate, certain conditions of equilibrium must be satisfied, i.e., side forces between the slices must be considered, or appropriate assumptions must be made concerning these side forces. Studies (10) show that the ordinary method of slices, which assumes that there are no side forces between slices, usually differs by less than 10%, on the conservative side, from more correct methods. When compared to the greater uncertainties associated with material heterogeneity, "minor" geological details, sampling, and testing, a less than 10% discrepancy seems relatively small. However, in exceptional cases, the ordinary method of slices can be in error by more than 35% (10).

Studies by Baligh and Azzouz (2) show that for a cohesive soil, consideration of end effects can lead to a 4%-40% increase in the factor of safety. Finite

Note.—Discussion open until February 1, 1978. To extend the closing date one month, a written request must be filed with the Editor of Technical Publications, ASCE. This paper is part of the copyrighted Journal of the Geotechnical Engineering Division, Proceedings of the American Society of Civil Engineers, Vol. 103, No. GT9, September, 1977. Manuscript was submitted for review for possible publication on October 19, 1976.

[1] Civ. Engr., Pacific Gas and Electric Co., San Francisco, Calif.

element studies of end effects by Lefebvre and Duncan (7) suggest that end effects become important for dams located in relatively narrow valleys with side slopes steeper than 3:1.

Previous investigations, as reviewed here, suggest that the assumption of two-dimensionality (plane strain) can not be justified without consideration of the specific problem to be solved. Errors associated with the assumption of two-dimensionality can be at least as large as errors associated with an inappropriate assumption regarding side forces between slices.

Previous methods of three-dimensional analysis are limited to cohesive soils and to specific cases. The studies described in the following sections present a general three-dimensional method of analysis by which any geometrical condition and any $c - \phi$ soil can be analyzed.

Theory

Definition of Factor of Safety.—The factor of safety, F, is often defined as the ratio of the summation of resisting forces to the summation of driving

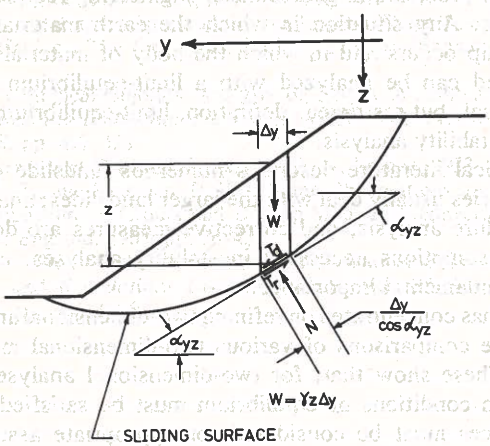

FIG. 1.—Section View of Two-Dimensional Slope Stability Analysis

forces along a shear surface. It can be shown that this definition is identical to one in which F = the ratio of the summation of strength to the summation of mobilized strength. The writer defines this same F as the ratio of the summation of available resistance to the summation of mobilized resistance along a shear surface:

$$F = \frac{\Sigma \text{ available resistance}}{\Sigma \text{ mobilized resistance}} \quad (1)$$

Two-Dimensional Factor of Safety, F_2.—The two-dimensional (2-D), or plane strain, case is shown in Fig. 1. For this case

$$F_2 = \frac{\Sigma (cA_2 + W_2 \cos \alpha_{yz} \tan \phi)}{\Sigma W_2 \sin \alpha_{yz}} \quad (2)$$

$$\text{or} \quad F_2 = \frac{\sum \left(\dfrac{c\Delta y}{\cos \alpha_{yz}} + \gamma z \Delta y \cos \alpha_{yz} \tan \phi \right)}{\Sigma \gamma z \Delta y \sin \alpha_{yz}} \quad (3)$$

per unit distance into the plane of the paper. In Eq. 3, cohesion c, friction angle ϕ, and density γ are variables; they can be functions of strain, confinement, pore pressure, tension cracks, and earth pressure. These considerations would be applied at each point along the shearing surface. If c, ϕ, γ, and Δy are constant, then

$$F_2 = \left(\frac{c}{\gamma}\right) \frac{\Sigma \sec \alpha_{yz}}{\Sigma z \sin \alpha_{yz}} + (\tan \phi) \frac{\Sigma z \cos \alpha_{yz}}{\Sigma z \sin \alpha_{yz}} \quad (4)$$

$$\text{or} \quad F_2 = \left(\frac{c}{\gamma h}\right) G_{c2} + \tan \phi \, G_{\phi 2} \quad (5)$$

The G_{c2} and $G_{\phi 2}$ terms are only functions of geometry. The G_{c2} term determines how cohesional resistance is influenced by geometry for a 2-D case, and the $G_{\phi 2}$ term determines how frictional resistance is influenced by geometry for a 2-D case. The height of the slope, h, can be taken outside the summation signs; the variable heights inside the summation signs are then z/h.

Three-Dimensional Factor of Safety, F_3.—Since 3-D analysis is uncommon, it may be helpful to begin with a typical 3-D slope instability problem (Fig. 2). A plan view with the contours is, except for a visit to the site and photographs of the landslide, often the first quantitative data provided. The direction of sliding may be somewhat curved depending on geological and topographic boundary constraints.

In setting up the problem (Fig. 3), a right-handed orthogonal coordinate system is selected. The y-coordinate direction is selected to be parallel to the direction of downslope movement. The x- and y-coordinates are perpendicular and are in the horizontal plane; and they are also perpendicular to the z-coordinate direction, which is vertical.

A single soil column, analogous to a slice in a 2-D analysis, is also shown in Fig. 3. Plan and section views of this soil column are shown in Fig. 4. The area of the soil column in the horizontal plane is defined by Δx and Δy, which can be selected directly on the topographic map. The inclination of the shearing surface is defined by the dip angles, α_{xz} in the x-z and α_{yz} in the y-z plane.

A 3-D view of the soil column is shown in Fig. 5. The following analysis, then, assumes that the soil column is selected small enough so that all faces can be described by straight lines. The top surface of the column may be irregular, but that is assumed to be relatively unimportant to the analysis; the depth of the column, z, is simply computed approximately from the center of the top face to the center of the bottom face (the shear surface).

Strike and dip of the shear surface follow the usual geological definition. It is necessary to derive a general expression for the dip angle (DIP) since it is needed to compute the normal force. Note also that, as a normal view is taken of the shear surface, a relatively regular area in the x-y plane is distorted, and the x and y-axes projected on the shear surface are not orthogonal. It is necessary to define angle θ, and to derive a general expression for the area of the shear surface, for the purpose of computing the cohesion acting on the surface.

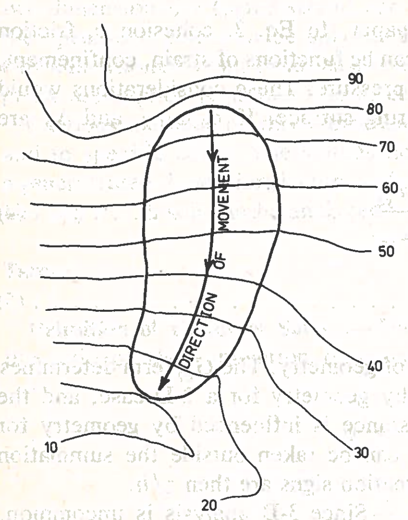

FIG. 2.—Plan View and Topography of Landslide

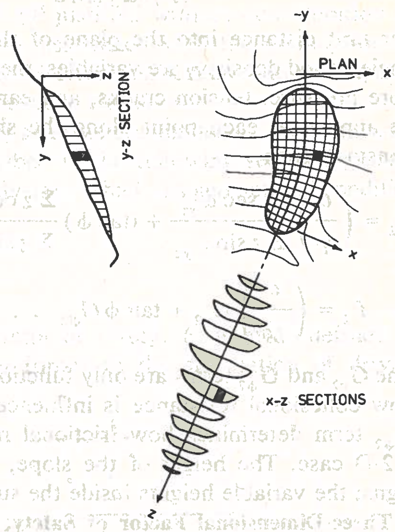

FIG. 3.—Coordinates, Plan, and Section Views of Landslide

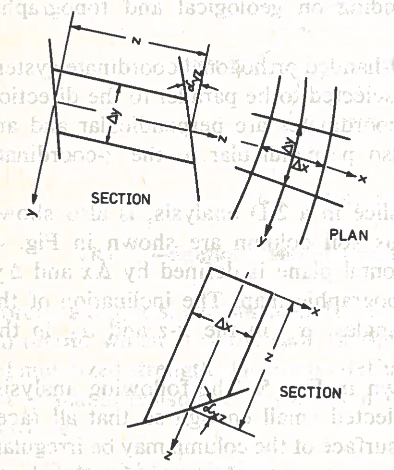

FIG. 4.—Plan and Section Views of One Soil Column

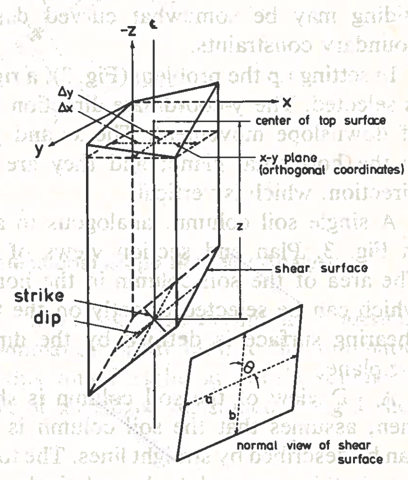

FIG. 5.—Three-Dimensional View of One Soil Column

The intersection of the axes with a portion of the lower corner of the shear surface shown in Fig. 5 is shown in Fig. 6. This is a three-dimensional view of an irregular cone bounded by the shear surface (on top), and the orthogonal

coordinate axes planes. The intersection of the shear surface with the horizontal plane is the strike line, and the local strike angle (STR) is defined as the angle between the strike line and the *y*-axis in the horizontal plane. The dip angle (DIP) defines the direction of the normal to the shear surface.

Using the terminology introduced with Fig. 6, an expression can be derived for (STR) as follows:

$$\sin(\text{STR}) = \frac{e}{f} = \frac{\dfrac{c'}{\tan\alpha_{xz}}}{\sqrt{e^2+d^2}} = \frac{\dfrac{c'}{\tan\alpha_{xz}}}{\sqrt{\left(\dfrac{c'}{\tan\alpha_{xz}}\right)^2+\left(\dfrac{c'}{\tan\alpha_{yz}}\right)^2}} \quad \ldots\ldots\ldots (6)$$

$$\sin(\text{STR}) = \left[1+\left(\frac{\tan^2\alpha_{xz}}{\tan^2\alpha_{yz}}\right)\right]^{-1/2} \quad \ldots\ldots\ldots (7)$$

Checking of Eq. 7 suggests that it is generally valid; i.e., if $\alpha_{xz} = \alpha_{yz}$, for any value of $0 < \alpha < 90°$, (STR) = 45°.

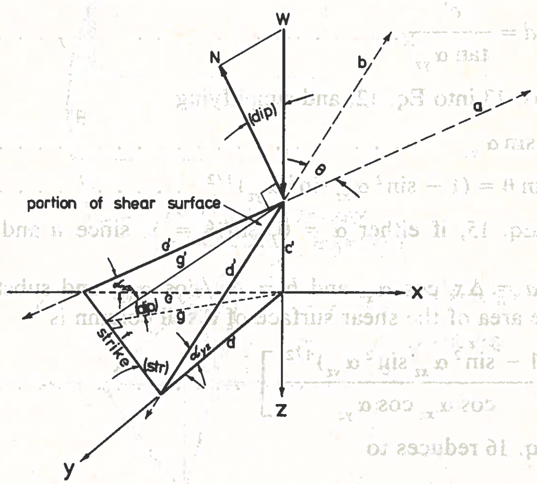

FIG. 6.—Three-Dimensional View of Portion of Shear Surface of Soil Column [Setup for Deriving Expressions for (STR), (DIP), and θ]

Similarly, a general expression can be derived for (DIP) as follows:

$$\cos(\text{DIP}) = \frac{g}{g'} = \frac{d\sin(\text{STR})}{\dfrac{c'}{\sin(\text{DIP})}} = \frac{\left(\dfrac{c'}{\tan\alpha_{yz}}\right)\sin(\text{STR})}{\dfrac{c'}{\sin(\text{DIP})}}$$

$$= \frac{\sin(\text{DIP})\sin(\text{STR})}{\tan\alpha_{yz}} \quad \ldots\ldots\ldots (8)$$

$$\cos(\mathrm{DIP}) = (1 + \tan^2\alpha_{xz} + \tan^2\alpha_{yz})^{-1/2} \qquad (9)$$

If $\alpha_{xz} = 0$, (DIP) $= \alpha_{yz}$, which is the often considered two-dimensional case. The normal force, N, equals $W\cos(\mathrm{DIP})$, or

$$N = W(1 + \tan^2\alpha_{xz} + \tan^2\alpha_{yz})^{-1/2} \qquad (10)$$

To compute the area of the shear surface of the soil column, it can be shown that the area of a general quadrilateral, A_3 (Figs. 5 and 6), is

$$A_3 = ab\sin\theta \qquad (11)$$

Again, using the terminology in Fig. 6, an expression is derived for θ. From the cosine law

$$\cos\theta = \frac{1}{2}\left(\frac{e'}{d'} + \frac{d'}{e'} - \frac{f^2}{e'd'}\right) \qquad (12)$$

and $e' = \dfrac{c'}{\sin\alpha_{xz}}$; $d' = \dfrac{c'}{\sin\alpha_{yz}}$; $f^2 = e^2 + d^2$;

$$e = \frac{c'}{\tan\alpha_{xz}}; \quad d = \frac{c'}{\tan\alpha_{yz}} \qquad (13)$$

Substituting Eqs. 13 into Eq. 12, and simplifying

$$\cos\theta = \sin\alpha_{xz}\sin\alpha_{yz} \qquad (14)$$

from which $\sin\theta = (1 - \sin^2\alpha_{xz}\sin^2\alpha_{yz})^{1/2}$ (15)

As shown by Eq. 15, if either $\alpha = 0$, $\sin\theta = 1$, since a and b intersect at 90°.

Noting that $a = \Delta x/\cos\alpha_{xz}$ and $b = \Delta y/\cos\alpha_{yz}$, and substituting Eq. 15 into Eq. 11, the area of the shear surface of a soil column is

$$A_3 = \Delta x\Delta y\left[\frac{(1 - \sin^2\alpha_{xz}\sin^2\alpha_{yz})^{1/2}}{\cos\alpha_{xz}\cos\alpha_{yz}}\right] \qquad (16)$$

For $\alpha_{xz} = 0$, Eq. 16 reduces to

$$A_3 = \frac{\Delta y}{\cos\alpha_{yz}}(\Delta x) \qquad (17)$$

which is the expression for 2-D analysis (Eq. 3) per unit distance Δx into the plane of the paper.

The preceding equations solve all quantities needed for the evaluation of F for soil columns which have in plan, a cross section of a general quadrilateral. Close to the boundary of the landslide (Fig. 7), there will always be some soil columns or elements that do not fall into this category. Two alternative approaches can be taken:

1. The boundary elements can be subdivided in plan into quadrilaterals (usually squares and rectangles) and triangles until the triangles are small enough to be neglected. The previously developed equations would apply to all elements that are quadrilateral in a plan view. This approach would probably be preferable for computer solution of the problem. Anticipated tension cracks should also be considered in deciding the sizes of triangular elements that should be neglected.

2. The triangular boundary soil elements can be considered separately. This approach appears to be preferable for long-hand computations.

Considering the soil elements shown in Fig. 7, elements A and B could be evaluated with the previously presented equations by approximating the boundary with the dashed lines parallel to direction y. Elements D and E, for example, would also be evaluated with the previously presented equations, with Δx and Δy defined as shown in Fig. 7(b). For element C, triangular in plan, with Δx, Δy, and z' defined as shown in Fig. 7(b), would have

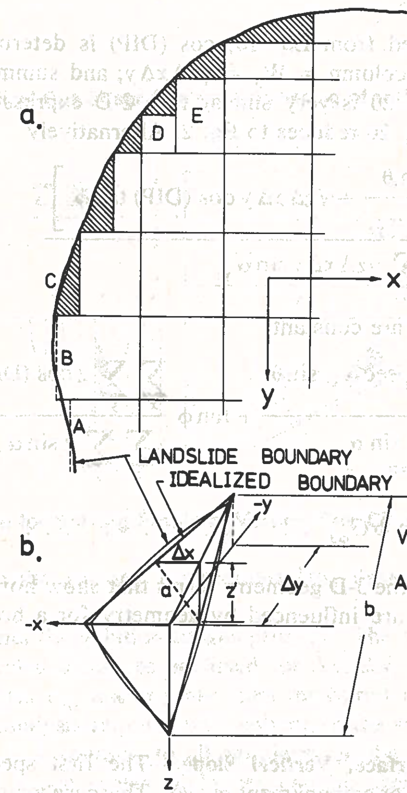

FIG. 7.—Boundary Soil Columns or Elements

$$W_3 = \frac{2}{3}(\gamma\Delta x\Delta y z') \qquad (18)$$

and the area would be computed from Eq. 11, in which a and b are defined as in Fig. 7(b), and $\sin\theta$ is defined by Eq. 15.

Sliding is assumed to occur only in direction y. The tangential driving forces are, therefore, only a function of α_{yz}:

$$T_D = W \sin \alpha_{yz} \quad (19)$$

Assuming that the vertical sides of the soil columns are frictionless (no side forces on the vertical sides of the soil columns, or with their influence canceling out, as for the 2-D analysis expressed by Eq. 2), a 3-D factor of safety can now be expressed as

$$F_3 = \frac{\sum_x \sum_y [cA_3 + W_3 \cos(\text{DIP}) \tan\phi]}{\sum_x \sum_y W_3 \sin \alpha_{yz}} \quad (20)$$

in which A_3 is determined from Eq. 16; cos (DIP) is determined from Eq. 9; the weight of any soil column = $W_3 = \gamma z \Delta x \Delta y$; and summation is carried out in both x and y. Eq. 20 is very similar to a 2-D expression for F, and, as shown, for $\alpha_{xz} = 0$, Eq. 20 reduces to Eq. 2. Alternatively

$$F_3 = \frac{\sum_x \sum_y \left[\frac{c \Delta x \Delta y \sin\theta}{\cos\alpha_{xz} \cos\alpha_{yz}} + \gamma z \Delta x \Delta y \cos(\text{DIP}) \tan\phi\right]}{\sum_x \sum_y \gamma z \Delta x \Delta y \sin\alpha_{yz}} \quad (21)$$

If c, ϕ, γ, and Δx and Δy are constant

$$F_3 = \left(\frac{c}{\gamma}\right) \frac{\sum_x \sum_y \sec\alpha_{xz} \sec\alpha_{yz} \sin\theta}{\sum_x \sum_y z \sin\alpha_{yz}} + \tan\phi \frac{\sum_x \sum_y z \cos(\text{DIP})}{\sum_x \sum_y z \sin\alpha_{yz}} \quad (22)$$

or $$F_3 = \left(\frac{c}{\gamma h}\right) G_{c3} + \tan\phi \, G_{\phi 3} \quad (23)$$

in which G_{c3} and $G_{\phi 3}$ are the 3-D geometry terms that show how the cohesional and frictional resistances are influenced by geometry for a homogeneous soil slope.

Special Cases

Cone Shaped Shear Surface, Vertical Slope.—The first special case to be considered is a vertical cut or embankment in clay. This case would have practical significance in evaluating the stable height of a trench, for example. It was chosen primarily to demonstrate the application of the presented method and to make possible a comparison with the solution by Baligh and Azzouz (2).

A 3-D view of the problem is shown in Fig. 8. The analysis would begin by drawing to scale the plan and section views of the problem (Fig. 9). Next, the soil columns are selected and drawn in the plan view [Fig. 9(*a*)]. Sections are then drawn of all soil columns [Figs. 9(*b*) and 9(*c*)]. Since the accuracy of the analysis depends on the extent to which the shear surface is approximated by straight line segments, smaller soil columns are selected where the shear surface is steeply inclined. Once the *y*-*z* sections [Fig. 9(*b*)] have been plotted, the *x*-*z* sections [Fig. 9(*c*)] can be determined by cross plotting between Figs. 9(*a*) and 9(*b*). Next the projection of the soil column axes (a and b in Fig. 5) are drawn on the *y*-*z* and *x*-*z* sections [the dashed lines in Figs. 9(*b*) and 9(*c*)].

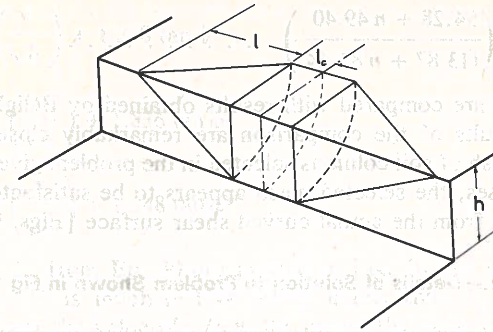

FIG. 8.—Vertical Cut Shear Surface Consisting of Circular Cylinder and Cone

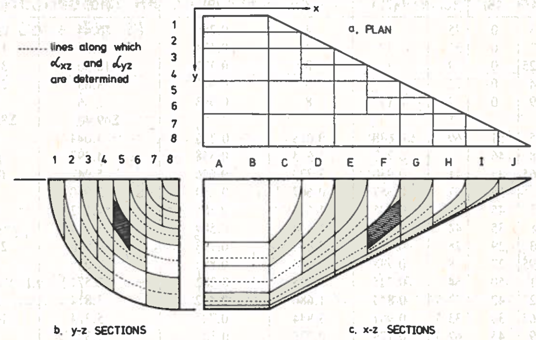

FIG. 9.—Setup for Solving Problem, Vertical Cut, Circular Cylinder, and Cone

Table 1 presents the solution to this problem. The soil columns are identified as indicated. Scaled distances are used for Δx, Δy, and z, as measured from Fig. 9. The angles α_{xz} and α_{yz} are then measured from Figs. 9(*b*) and 9(*c*). The rest of the analysis requires only solving of the simple equations.

The example is a solution to all problems of the same geometry, i.e., any height of slope (since scaled distances can be used) and any length of the cylindrical section. This can be expressed as

$$F_3 = \left(\frac{c}{\gamma h}\right)\left(\frac{94.28 + n\,49.40}{113.87 + n\,85.64}\right)\frac{1}{8} \quad (24)$$

in which n = fraction or number of 2-D sections, i.e.

$$G_{c2} = \left(\frac{49.40}{85.64}\right)\frac{1}{8} = 0.0721 \quad (25)$$

$$G_{c3} = \left(\frac{94.28 + n\,49.40}{113.87 + n\,85.64}\right)\frac{1}{8} \quad (26)$$

The ratio of the 3-D to the 2-D factor of safety can be expressed as

$$\frac{F_3}{F_2} = \frac{G_{c3}}{G_{c2}} = 1.733\left(\frac{94.28 + n\,49.40}{113.87 + n\,85.64}\right) \quad (27)$$

Results of Eq. 27 are compared with results obtained by Baligh and Azzouz (2) in Table 2. Results of the comparison are remarkably close, considering the rather coarse mesh of soil columns selected in the problem given as example. For practical purposes, the selected mesh appears to be satisfactory. Note the significant deviation from the actual curved shear surface [Figs. 9(*b*) and 9(*c*), Column F5] resulting from the planar approximation required by the theory presented here. For more accurate comparisons, a finer mesh is necessary, particularly where the shear surface is steeply inclined.

TABLE 1.—Details of Solution to Problem Shown in Fig. 8

Soil column (1)	Δx (2)	Δy (3)	z (4)	α_{xz} (5)	α_{yz} (6)	$\sin\theta = (1 - \sin^2\alpha_{xz}\sin^2\alpha_{yz})^{1/2}$ (7)	$\Delta x\Delta y\sin\theta$ (8)	$\cos\alpha_{xz}\cos\alpha_{yz}$ (9)	$\Delta x\Delta y\sin\theta/(\cos\alpha_{xz}\cos\alpha_{yz})$ (10)	$z\Delta x\Delta y\sin\alpha_{yz}$ (11)	$G_c = (1/8)/(\Sigma 10/\Sigma 11)$ (12)
AB1	4	1	2.3	0	75	1	4	0.259	15.44	8.89	
AB2	4	1	4.7	0	55	1	4	0.574	6.97	15.40	
AB34	4	2	6.25	0	39	1	8	0.777	10.30	31.47	
AB56	4	2	7.4	0	22	1	8	0.927	8.63	22.18	
AB78	4	2	7.9	0	7	1	8	0.993	8.06	7.70	
									Σ49.40	Σ85.64	0.0721
C1[a]	2	0.5	2.5	51	69	0.688	0.688	0.226	3.044	1.557	
C2	2	1	3.8	46	59	0.787	1.574	0.358	4.397	6.514	
C34	2	2	5.65	34	41	0.930	3.720	0.626	5.942	14.827	
D2[a]	2	0.5	2.2	54	67	0.667	0.667	0.230	2.900	1.351	
D3	2	1	3.5	45	57	0.805	1.610	0.385	4.182	5.871	
D4	2	1	4.8	35	44	0.917	1.834	0.589	3.114	6.669	
CD56	4	2	6.3	29	25	0.979	7.832	0.793	9.876	21.300	
CD78	4	2	6.95	27	8	0.998	7.984	0.882	9.052	7.738	
E3[a]	2	0.5	2.1	50	64	0.725	0.725	0.282	2.571	1.259	
E4	2	1	3.2	42	53.5	0.843	1.686	0.442	3.814	5.145	
E56	2	2	4.65	30	33.5	0.961	3.844	0.722	5.324	10.266	
F4[a]	2	0.5	1.9	45	62.5	0.779	0.779	0.327	2.382	1.124	
F5	2	1	2.9	40	49	0.874	1.748	0.503	3.475	4.377	
F6	2	1	3.8	31.5	33	0.959	1.918	0.715	2.683	4.139	
EF78	4	2	4.9	27	11	0.996	7.968	0.875	9.106	7.480	
G5[a]	2	0.5	1.7	44	60.5	0.797	0.797	0.354	2.251	0.987	
G6	2	1	2.45	37	44	0.908	1.816	0.574	3.164	3.404	
G78	2	2	3.35	27	17	0.991	3.964	0.852	4.653	3.918	
H6[a]	2	0.5	1.4	41	56	0.839	0.839	0.422	1.988	0.774	
H7	2	1	2.1	34	35	0.947	1.894	0.679	2.789	2.409	
H8	2	1	2.4	27	12	0.996	1.992	0.872	2.284	0.998	
I7[a]	2	0.5	1.0	37	46	0.901	0.901	0.555	1.623	0.480	
I8	2	1	1.3	30	20.5	0.985	1.970	0.811	2.429	0.911	
J8[a]	2	0.5	1.2	27	28	0.977	0.977	0.787	1.241	0.376	
									Σ94.28	Σ113.87	0.1035
									Σ143.68	Σ199.51	0.0900

[a]Col. 11 = (2/3) $z\Delta x\Delta y\sin\alpha_{yz}$.

Note: $\phi = 0$; $F_3 = \left(\dfrac{c}{\gamma}\right)\dfrac{\sum \dfrac{\Delta x\Delta y\sin\theta}{\cos\alpha_{xz}\cos\alpha_{yz}}}{\Sigma z\Delta x\Delta y\sin\alpha_{yz}} = \left(\dfrac{c}{\gamma h}\right)G_{c3}$.

It is of interest to consider a $c - \phi$ soil for the same sample problem. This requires the solution of $G_{\phi 3}$ of Eq. 23. The only term not already considered in Table 1 is the cos (DIP) term given by Eq. 9. Such calculations then give

$$F_3 = 0.1035\left(\frac{c}{\gamma h}\right) + 1.836\tan\phi \quad (28)$$

$$F_2 = 0.0721\left(\frac{c}{\gamma h}\right) + 1.248\tan\phi \quad (29)$$

$$\frac{F_3}{F_2} = \frac{0.1035\left(\dfrac{c}{\gamma h}\right) + 1.836\tan\phi}{0.0721\left(\dfrac{c}{\gamma h}\right) + 1.248\tan\phi} \quad (30)$$

Ratios of F_3/F_2 from Eq. 30 are plotted in Fig. 10. As shown, for a conical shear surface, F_3 is much (~1.44 times) higher than F_2 for all values of c and ϕ. The lower the value of $c/\gamma h$, the higher the value of F_3/F_2.

Wedge-Shaped Shear Surface.—Wedges have been analyzed previously in rock mechanics (4,6,8), but to the writer's knowledge, such analyses have not yet been applied to soil mechanics problems. Due to the simple geometry of the selected wedge, an independent "closed-form" solution was possible.

TABLE 2.—Comparison of Results, Vertical Cut in Clay, Shear Surface Consisting of Cylinder and Cone (Fig. 8)

Basis $l/h = 2$ (1)	F_3/F_2: $n = 0$, $l_c/h = 0$ (2)	$n = 1$, $l_c/h = 0.5$ (3)	$n = 2$, $l_c/h = 1$ (4)	$n = 4$, $l_c/h = 2$ (5)	$n = 8$, $l_c/h = 4$ (6)
Presented theory, Eq. 27	1.44	1.25	1.17	1.11	1.06
Baligh and Azzouz (2)	—	1.23	1.16	1.09	1.06

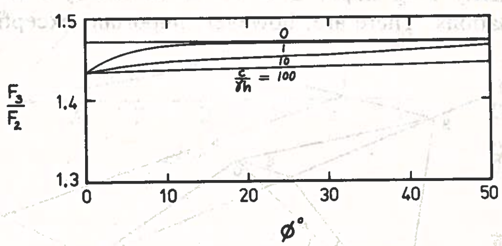

FIG. 10.—F_3/F_2 Ratios, Vertical Cut, Shear Surface Consisting of Circular Cylinder and Cone

The setup for the computation of the F for a three-dimensional wedge is shown in Fig. 11. Since sliding is considered possible only down the intersection of planes CAO and CBO, $T_D = W\sin i$, as for a two-dimensional wedge. However, the normal force, normal to planes CAO and CBO, can be computed using vector analysis:

$$\mathbf{N} = \mathbf{W} \times \left(\frac{\mathbf{OA} \times \mathbf{OC}}{|\mathbf{OA} \times \mathbf{OC}|}\right) \quad (31)$$

When all the vector quantities are resolved, and the necessary substitutions are made

$$F_3 = \frac{3c}{\gamma b'}\frac{B}{\sin i} + \frac{1}{B}\frac{\tan\phi}{\tan i} \quad \text{(32)}$$

in which $B = \left[4\left(\frac{b'}{w}\right)^2 \sin^2 i + 1\right]^{1/2}$ (33)

When the three-dimensional and the two-dimensional F values are expressed as a ratio

$$\frac{F_3}{F_2} = \frac{1.5B + \frac{1}{B}\frac{\gamma b'}{4c}\tan\phi \sin 2i}{1 + \frac{\gamma b'}{4c}\tan\phi \sin 2i} \quad \text{(34)}$$

Limiting Conditions.—For a cohesionless soil, $c = 0$

$$\frac{F_3}{F_2} = \frac{1}{B} \quad \text{(35)}$$

For a frictionless soil, $\phi = 0$

$$\frac{F_3}{F_2} = 1.5B \quad \text{(36)}$$

For an infinitely long slope, $B = 1$. As shown by Eq. 33, B is close to 1 for most situations. There are, however, important exceptions. Consider the

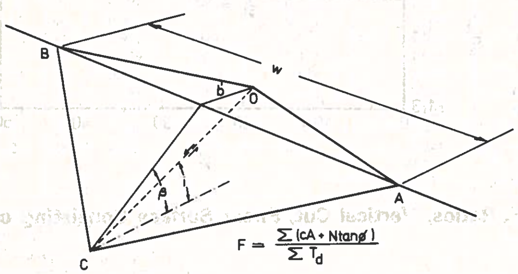

FIG. 11.—Three-Dimensional Wedge

stability of a vertical open trench in a sandy soil; assume $c = 0$. As indicated by Eqs. 33 and 35, the narrower the wedge (the smaller b'/w), the lower the factor of safety. With $b'/w = 1/2$ and $i = 45°$, $F_3/F_2 = 0.816$. These studies, then, indicate that narrow wedge-shaped failures are more likely in a sandy soil, and that some extreme situations may have significantly less stability than that determined from 2-D analyses.

Eq. 34 can also be expressed as a function of the slope height h by observing from Fig. 11 that

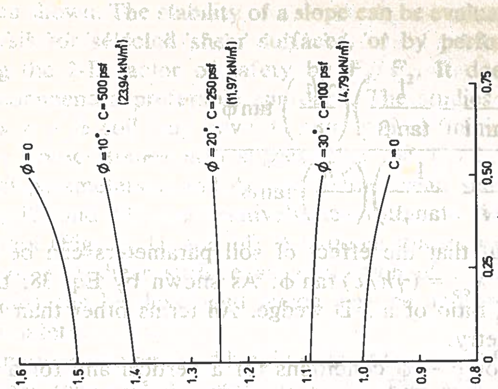

FIG. 14.—Effect of b'/w, Wedge, 2:1 Slope [$i = 18.4°$, $\gamma = 100$ pcf (1,602 kg/m³), $b' = 50$ ft (15 m)]

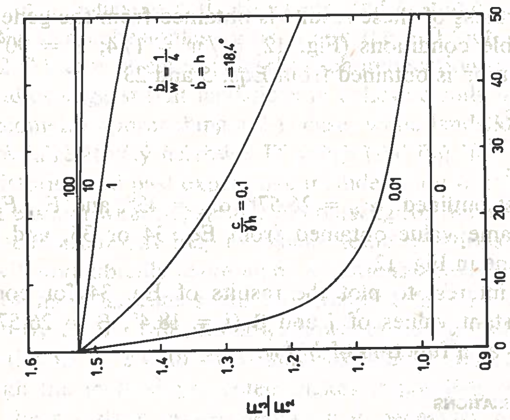

FIG. 13.—F_3/F_2 Ratios, Wedge, 2:1 Slope

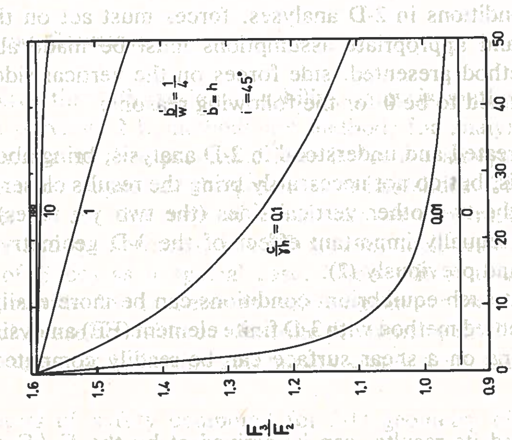

FIG. 12.—F_3/F_2 Ratios, Wedge, Vertical Slope

$$\frac{b'}{h} = \frac{1}{\tan i} - \frac{1}{\tan \beta} \quad (37)$$

$$\frac{F_3}{F_2} = \frac{1.5B + \dfrac{\sin 2i}{4B}\left(\dfrac{1}{\tan i} - \dfrac{1}{\tan \beta}\right)\left(\dfrac{\gamma h}{c}\right)\tan \phi}{1 + \dfrac{\sin 2i}{4}\left(\dfrac{1}{\tan i} - \dfrac{1}{\tan \beta}\right)\left(\dfrac{\gamma h}{c}\right)\tan \phi} \quad (38)$$

Janbu (5) pointed out that the effect of soil parameters can be expressed by a single parameter, $\lambda_{c\phi} = (\gamma h/c) \tan \phi$. As shown by Eq. 38, this is also possible for the F_3/F_2 ratio of a 3-D wedge. All terms other than $\lambda_{c\phi}$ in Eq. 38 deal only with geometry.

Eq. 38 was solved for $c - \phi$ conditions for a vertical and for a 2:1 slope; the results are presented in Figs. 12 and 13. The significance of differences in geometry becomes clear when Figs. 12 and 13 are compared with Fig. 10. For wedges (Figs. 12 and 13), the lowest F_3/F_2 ratios are obtained for $c/\gamma h = 0$; for cones, the lowest F_3/F_2 ratios are obtained for high values of $c/\gamma h$. A check on the correctness of these results is obtained from the general theory, Eq. 22. For comparable conditions (Fig. 12, $b'/w = 1/4$, $\beta = 90°$, $b' = h$, $i = 45°$), an exact solution is obtained from Eqs. 5 and 23:

$$\frac{F_3}{F_2} = \frac{G_{\phi 3}}{G_{\phi 2}} = \frac{\cos(\text{DIP})}{\cos \alpha_{yz}} \quad (39)$$

For the conditions just outlined, $\alpha_{xz} = 26.57°$, $\alpha_{yz} = 45°$, and $F_3/F_2 = 0.943$. This is exactly the same value obtained from Eq. 34 or 35, and plotted as the lower horizontal line in Fig. 12.

It may also be of interest to plot the results of Eq. 34 for combinations of c and ϕ. For constant values of i and β ($i = 18.4°$, $\beta = 26.57°$), F_3/F_2 is presented in Fig. 14 as a function of b'/w.

Considerations and Implications

It is generally known, as was pointed out by Bishop (3), that in order to satisfy equilibrium conditions in 2-D analyses, forces must act on the vertical sides of each slice, and appropriate assumptions must be made about these forces. In the 3-D method presented, side forces on the vertical sides of each soil column were assumed to be 0 for the following reasons:

1. Side forces, as treated and understood in 2-D analysis, bring about a more acceptable 2-D analysis, but do not necessarily bring the results closer to reality, since side forces on the two other vertical sides (the two y-z faces) have not been considered. The equally important effect of the 3-D geometry has been demonstrated herein and previously (2).
2. It is believed that such equilibrium conditions can be more easily satisfied by combining the presented method with 3-D finite element (FE) analysis. Stresses and deformations acting on a shear surface can be readily computed with the FE method.

The 3-D method, and its results, can be arrived at by the F_3/F_2 ratio also, as has been shown. The stability of a slope can be evaluated by either performing 3-D analysis for selected shear surfaces, or by performing 2-D analysis and correcting the 2-D factor of safety by F_3/F_2. It does not appear advisable yet to recommend a preferable approach. The studies reported herein suggest that every $c - \phi$ soil may have its own critical (minimum) shear surface and geometry. These studies also suggest that the F_3/F_2 ratio is quite sensitive to the soil parameters c and ϕ, and to the basic shape of the shear surface (Figs. 10, 12, and 13), but relatively insensitive to the width (1 or w) of the shear surface (Figs. 8, 11, and 14). Additional studies are necessary to determine the type of 3-D shear surface as a function of c and ϕ. On such a basis, F_3/F_2 ratios can be developed which may be appropriate for modifying 2-D factors of safety.

Preliminary results reported herein suggest that a 3-D factor of safety is usually much higher than a 2-D factor of safety. End effects alone cannot explain this increase. In going from a 2-D to a 3-D situation, at least for a cohesive soil, driving forces are reduced by a distance cubed, while resisting forces are reduced by a distance squared. The end result is more stability for any 3-D case in a cohesive soil. However, these studies also suggest that there are situations in cohesionless soils where the 3-D factor of safety may be less than the 2-D factor of safety; clearly such implications warrant careful scrutiny.

The studies suggest that landslides in cohesive soils may follow a wide shear surface geometry approaching a 2-D case, while landslides in cohesionless soils may follow a relatively narrow 3-D wedge (see Fig. 14).

Case histories and past experience include many situations where calculations could not explain what happened. Accounting for the 3-D nature of the problem as presented herein may help to explain some situations; i.e., possibly Resendiz (9), but will undoubtedly leave many situations unexplained. The in-situ characteristics of most landslides are too complex for any simple explanations. A correction by F_3/F_2 will probably, however, bring total (low ϕ, higher c) and effective (higher ϕ, $c \cong 0$) stress analysis to closer agreement.

Although the method presented makes it possible to describe and analyze any 3-D shear surface, experimentation is necessary to find the critical shear surface, just as it is in 2-D analyses.

Summary and Conclusions

A general three-dimensional stability analysis method has been presented. While all previous 2-D methods are methods for analysis of cross sections of landslides, the method presented here is for the analysis of landslides and for the analysis of slopes for the potential of landslides. The apparent correctness and generality of the method have been demonstrated by selected limiting conditions and special cases. The 3-D solution includes within it the 2-D Ordinary Method of Slices as a special case. The method assumes that there are no equilibrium side forces between soil columns or that their influence cancels out. Special cases considered illustrate preliminary implications of 3-D analyses. On such bases the following preliminary conclusions may be made:

1. Factors of safety computed for 3-D geometry differ considerably from ordinary 2-D factors of safety.

2. Three-dimensional factors of safety are generally much higher than 2-D factors of safety. However, situations appear to exist where the 3-D factor of safety can be lower than the 2-D factor of safety.

3. The F_3/F_2 ratio appears to be quite sensitive to c and ϕ and to the shape of the 3-D shear surface.

General expressions are also derived for strike and dip; if the inclination of a plane is given in two orthogonal directions, strike and dip can be determined.

Appendix.—References

1. "Advances in Rock Mechanics," *Proceedings of the Third International Society for Rock Mechanics Congress*, Vol. II-b, 1974.
2. Baligh, M. M., and Azzouz, A. S., "End Effects on Stability of Cohesive Slopes," *Journal of the Geotechnical Engineering Division*, ASCE, Vol. 101, No. GT11, Proc. Paper 11705, Nov., 1975, pp. 1105-1117.
3. Bishop, A. W., "The Use of the Slip Circle in the Stability Analysis of Slopes," *Geotechnique*, London, England, Vol. 5, No. 1, Mar., 1955, pp. 7-17.
4. Hamel, J. V., "Rock Strength From Failure Cases: Left Bank Slope Stability Study, Libby Dam and Lake Koocanusa, Montana," *Technical Report MRD-1-74*, U.S. Army Corps of Engineers, Missouri River Division, Omaha, Neb., July, 1974.
5. Janbu, N., "Earth Pressure and Bearing Capacity Calculations by Generalized Procedure of Slices," *Proceedings of the Fourth International Conference on Soil Mechanics and Foundation Engineering*, Vol. 2, London, England, 1957, pp. 207-212.
6. John, K. W., "Graphical Stability Analysis of Slopes in Jointed Rock," *Journal of the Soil Mechanics and Foundations Division*, ASCE, Vol. 94, No. SM2, Proc. Paper 5865, Mar., 1968, pp. 497-526.
7. Lefebvre, G., and Duncan, J. M., "Three-Dimensional Finite Element Analyses of Dams," *Journal of the Soil Mechanics and Foundations Division*, ASCE, Vol. 99, No. SM7, Proc. Paper 9857, July, 1973, pp. 495-507.
8. Londe, P., *A Three-Dimensional Method of Analysis for Rock Slopes*, Coyne & Bellier, Paris, France, 1964.
9. Resendiz, D., discussion of "Accuracy of Equilibrium Slope Stability Analysis," by S. G. Wright, F. H. Kulhawy, and J. M. Duncan, *Journal of the Soil Mechanics and Foundations Division*, ASCE, Vol. 99, No. SM10, Proc. Paper 10097, Oct., 1973, pp. 783-791.
10. Wright, S. G., "A Study of Slope Stability and the Undrained Shear Strength of Clay Shales," thesis presented to the University of California, at Berkeley, Calif., in 1969, in partial fulfillment of the requirements for the degree of Doctor of Philosophy.
11. Wright, S. G., Kulhawy, F. H., and Duncan, J. M., "Accuracy of Equilibrium Slope Stability Analysis," *Journal of the Soil Mechanics and Foundations Division*, ASCE, Vol. 99, No. SM10, Proc. Paper 10097, Oct., 1973, pp. 783-791.

JOURNAL OF THE GEOTECHNICAL ENGINEERING DIVISION

Slabjacking—State-of-the-Art

By the Committee on Grouting of the Geotechnical Engineering Division

Introduction

This paper is one of a series of current state-of-the-art reports sponsored by the Committee on Grouting. Its scope is limited to the raising of concrete pavements, formerly known as "mudjacking," and stabilization of slabs by filling existing under-slab voids. Pressure grouting techniques for stabilization or impermeabilization of soils or rock at some depth below the surface of the ground are not included.

Pressure injection for the purpose of raising or stabilizing faulty concrete pavement has been practiced for more than 40 years. During this period a variety of different materials have been utilized including hot asphalt, various soil and soil-cement slurries, and a wide variety of cement and cement-sand grouts. Historically, such materials have been mixed into slurries or pourable fluids, often described as having the appearance of "cream." Over the years a great deal of research and a large amount of actual work has been performed. However, due to limitations in the various systems and equipment, the full potential of the methods has only come to realization within the past decade or so. Equipment and techniques for this type of work have now become highly developed, enabling the knowledgeable engineer to obtain nearly any desired result, be it the simple filling of under-slab voids or the precise lifting and leveling of virtually any concrete slab or rigid pavement. The technique as presently practiced is properly referred to as "slabjacking" when lifting or leveling is involved, or simply "pressure grouting" where void filling is the sole objective. Although the term "Mudjacking" has been used extensively in the past due to the practice of using the "Mudjack" machine, the term is now considered inappropriate as modern practice involves many types of machinery and materials.

The purpose of this paper is to acquaint the reader with the present state-of-the-

Note.—Discussion open until February 1, 1978. To extend the closing date one month, a written request must be filed with the Editor of Technical Publications, ASCE. This paper is part of the copyrighted Journal of the Geotechnical Engineering Division, Proceedings of the American Society of Civil Engineers, Vol. 103, No. GT9, September, 1977. Manuscript was submitted for review for possible publication on January 25, 1977.

VOL. 104 NO. GT9. SEPT. 1978

JOURNAL OF THE GEOTECHNICAL ENGINEERING DIVISION

PROCEEDINGS OF THE AMERICAN SOCIETY OF CIVIL ENGINEERS

AMERICAN SOCIETY OF CIVIL ENGINEERS FOUNDED 1852

VOL.104 NO.GT9. SEPT. 1978

JOURNAL OF THE GEOTECHNICAL ENGINEERING DIVISION

PROCEEDINGS OF THE AMERICAN SOCIETY OF CIVIL ENGINEERS

CONTENTS

DISCUSSION

Proc. Paper 13978

→

This Journal is published monthly by the American Society of Civil Engineers. Publications office is at 345 East 47th Street, New York, N.Y. 10017. Address all ASCE correspondence to the Editorial and General Offices at 345 East 47th Street, New York, N.Y. 10017. Allow six weeks for change of address to become effective. Subscription price to members is $12.00. Nonmember subscriptions available; prices obtainable on request. Second-class postage paid at New York, N.Y. and at additional mailing offices. GT, HY.

[a]Discussion period closed for this paper. Any other discussion received during this discussion period will be published in subsequent Journals.

13999 USE OF PILES AS ISOLATION BARRIERS

KEY WORDS: **Acoustic properties;** Acoustics; Dynamic structural analysis; Geotechnical engineering; **Isolation; Piles (foundations);** Soil dynamics; **Vibration**

ABSTRACT: An acoustic model employing sound waves in a fluid medium was used to evaluate the use of rows of piles as passive isolation barriers to reduce ground vibrations. The results of experimental measurements indicate that the effectiveness of the barriers is highly dependent on the mismatch between pile and soil material properties, with greater mismatch resulting in greater effectiveness. Pile-to-pile aperture spacing of 0.4 times the wavelength was found to be the upper bound for a barrier to have some effectiveness, and a minor dependence of effectiveness on the pile diameter was also observed. The extrapolation of the model studies to actual field problems is considered.

REFERENCE: Liao, Samson, and Sangrey, Dwight A., "Use of Piles as Isolation Barriers," *Journal of the Geotechnical Engineering Division,* ASCE, Vol. 104, No. GT9, **Proc. Paper 13999**, September, 1978, pp. 1139-1152

14040 DEFORMATION, STRENGTH OF SOFT BANGKOK CLAY

KEY WORDS: **Clays;** Consolidation; **Deformation; Shear strength; Thailand;** Triaxial tests

ABSTRACT: A comprehensive series of stress controlled triaxial compression tests was carried out on Soft Bangkok Clay. Undisturbed samples of soft clay were taken from Nong Ngoo Hao, a site situated about 15 km east of the coast in the Chao Phraya Plain. Altogether, four different types of triaxial tests were carried out and these include: (1)Undrained tests with constant cell pressure and with 1-hr and 1-day load increment durations; (2)fully drained tests with constant cell pressure; (3)constant mean normal stress tests under drained conditions; and (4)anisotropic consolidation tests. The experimentally observed stress-strain behavior is compared with the predictions from various stress-strain theories.

REFERENCE: Balasubramaniam, A. S., and Chaudry, A. R., "Deformation and Strength Characteristics of Soft Bangkok Clay," *Journal of the Geotechnical Engineering Division,* ASCE, Vol. 104, No. GT9, **Proc. Paper 14040**, September, 1978, pp. 1153-1167

14042 FOUNDATION GROUTING AT MOULAY YOUSSEF DAM

KEY WORDS: **Dam foundations; Dams;** Drains; Economic analysis; **Foundation grouting;** Grout; Grouting; **Morocco;** Piezometers; Seepage

ABSTRACT: A rational "wait-and-see" approach to the problem of foundation treatment was developed for Moulay Youssef Dam in Morocco to keep costs down while not decreasing the safety of the structure in any way. This was to carry out a minimum of initial grouting, install piezometers and drains in the foundation, and provide a control tunnel from which problem areas could be identified and given additional treatment after filling if necessary. When Moulay Youssef Dam was filling for the first time, discharge from one of the drains on the right bank increased suddenly giving cause for alarm. Reservoir filling was stopped and further drains were drilled. A wet zone in the control tunnel enabled the suspect area to be localized and heavily grouted, which reduced the seepage to an acceptable level. The main work was done from the control tunnel. Despite the additional works, the final cost was considerably less than the estimate for the traditioonal foundation treatment.

REFERENCE: Benzekri, Mehdi, and Marchand, Rene J., "Foundation Grouting at Moulay Youssef Dam," *Journal of the Geotechnical Engineering Division,* ASCE, Vol. 104, No. GT9, **Proc. Paper 14042**, September, 1978, pp. 1169-1181 shear strength, even though the former limits the maximum particle size to No. 4 sieve (4.76 mm) while the latter to 3/4 in. (19.1 mm).

Appendix.—References

7. Huang, Y. H., "Stability of Spoil Banks and Hollow Fills Created by Surface Mining," *Report No. IMMR34-RRR1-78*, Institute for Mining and Minerals Research, University of Kentucky, Lexington, Ky., Mar., 1978.

Three-Dimensional Slope Stability Analysis Method[a]

Discussion by Amr S. Azzouz,[2] A. M. ASCE and Mohsen M. Baligh,[3] M. ASCE

The author presented a general three-dimensional, 3-D, method for slope stability analysis. Results obtained from a similar study performed at the Massachusetts Institute of Technology (2,12,14) raise two major issues.

Normal Stress on Shear Surface.—Based on the ordinary method of slices (OMS) (13), and in order to achieve statical determinancy, the author neglected the forces on all four vertical sides of soil columns. This simplification may be reasonable for some two-dimensional, 2-D, problems, but is unacceptable for evaluating the 3-D stability of frictional slopes ($\phi \neq 0$). This is shown in Fig. 15, where the OMS was used to study the 3-D stability of homogeneous slopes employing the shear surfaces of revolution described in Ref. 2. In Fig. 15, the end effects parameter, F_3/F_2, is plotted versus the normalized total failure width, $2L/DR$ [$2L = 2(l + l_c)$ in Fig. 8]. F_3 is the minimum 3-D factor of safety for different types of shear surfaces (ellipsoids and cones attached to cylinders of different widths) and F_2 is the plane strain factor of safety; $\lambda_{c\phi}$ and DR are defined in Fig. 15. The details of the analysis are given in Ref. 12. Fig. 15 shows the following.

1. End effects increase as $\lambda_{c\phi}$ decreases. This contradicts the results in Fig. 10 where, for a fixed value of $c/\gamma h$, the ratio F_3/F_2 increases as ϕ increases. This discrepancy is believed to be due to either computational errors or to insufficient search for the minimum value of F_3 in the author's analysis. To illustrate the importance of the search for a minimum value of F_3, consider slopes with $c = 0$. For cylindrical shear surfaces with vertical end sections, the OMS gives $F_3/F_2 = 1$ because the method neglects the shear resistance on the two vertical end sections. Thus, the value of $F_3/F_2 = 1.47$ obtained

[a] September, 1977, by H. John Hovland (Proc. Paper 13221).
[2] Research Assoc., Massachusetts Inst. of Tech., Cambridge, Mass.
[3] Assoc. Prof. of Civ. Engrg., Massachusetts Inst. of Tech., Cambridge, Mass.

by the author using the OMS for conical shear surfaces can be misleading and erroneous if used in design.

2. For highly frictional slopes ($\lambda_{c\phi} = 100$), F_3/F_2 is less than unity and the critical failure width is very narrow. The OMS thus predicts that the failure of frictional slopes takes place along very narrow and deep failures contrary to typical observed failure modes. This discrepancy arises because the OMS underestimates the frictional resistance on steep shear surfaces (DIP → 90°,

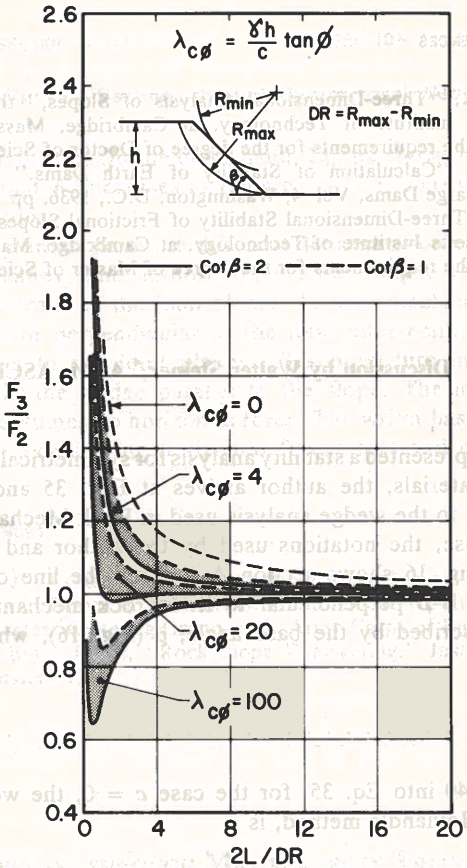

FIG. 15.—Results of Stability Analysis of Homogeneous Slopes According to Ordinary Method of Slices

Eq. 20). In fact, as c tends to zero ($\lambda_{c\phi} \to \infty$), the critical failure mode consists of very deep and narrow shear surfaces and F_3 approaches zero. This is clearly demonstrated by Eq. 35, for wedge-shaped shear surfaces, when w tends to zero, i.e., the OMS predicts that all sandy slopes, irrespective of their inclinations, are unstable. This is clearly unrealistic.

Effect of Width of Failure on F_3/F_2.—The author states that "the ratio F_3/F_2 is relatively insensitive to the width of the shear surface." Fig. 15, which is based on the OMS used by the author, contradicts this conclusion if the width of the shear surface is defined as $2L = 2(l + l_c)$ (Fig. 8). Moreover, if the width refers to the length of the cone, l, results obtained by the writers in 1975 (2) and by the closed-form solution for $\phi = 0$ (12) also disagree with the preceding statement.

In conclusion, the OMS is inadequate for the 3-D analysis of frictional slopes and a method taking into consideration the side forces on vertical planes is required. Such a method will be presented in a subsequent article in this journal.

Appendix.—References

12. Azzouz, A. S., "Three-Dimensional Analysis of Slopes," thesis presented to the Massachusetts Institute of Technology, at Cambridge, Mass., in 1977, in partial fulfillment of the requirements for the degree of Doctor of Science.
13. Fellenius, W., "Calculation of Stability of Earth Dams," *Transactions,* Second Congress on Large Dams, Vol. 4, Washington, D.C., 1936, pp. 445–459.
14. Steiner, W., "Three-Dimensional Stability of Frictional Slopes," thesis presented to the Massachusetts Institute of Technology, at Cambridge, Mass., in 1977, in partial fulfillment of the requirements for the degree of Master of Science.

Discussion by Walter Steiner,[4] A. M. ASCE

The author has presented a stability analysis for symmetrical tetrahedral wedges. For frictional materials, the author arrives at Eqs. 35 and 39. These results will be compared to the wedge analysis used in Rock Mechanics (15,16).

For this purpose, the notations used by the author and in rock mechanics are compared. Fig. 16 shows section A-A along the line of joint intersection O-C and section B-B perpendicular to it. In rock mechanics, the opening of the wedge is described by the base angle, ρ (Fig. 16), which is related to B in Eq. 33 by

$$B = \frac{1}{\cos\rho} \qquad (40)$$

substituting Eq. 40 into Eq. 35, for the case $c = 0$, the wedge factor F_3/F_2, as predicted by Hovland's method, is

$$\frac{F_3}{F_2} = \cos\rho \qquad (41)$$

In rock mechanics analysis (15,16), the wedgefactor is

$$\frac{F_3}{F_2} = \frac{1}{\cos\rho} \qquad (42)$$

Comparing Eqs. 41 and 42, one sees that the author's result (Eq. 41) predicts that the three-dimensional factor of safety tends to zero when ρ approaches 90°, i.e., all cohesionless slopes ($c = 0$) are unstable against deep failure modes.

[4] Research Asst., Dept. of Civ. Engrg., Massachusetts Inst. of Tech., Cambridge, Mass.

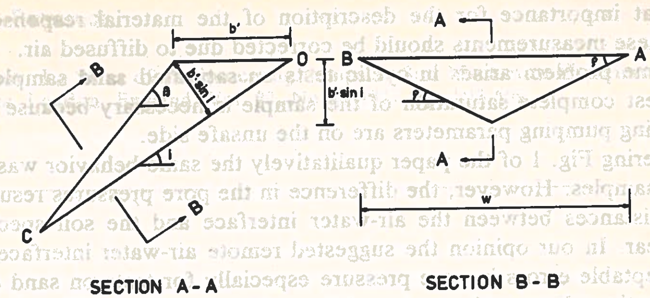

FIG. 16.—Sections through Symmetrical Wedge

This is clearly unrealistic. On the other hand, Eq. 42 shows that rock mechanics analysis predicts that F_3 increases as ρ increases, i.e., narrow wedges are more stable than wide ones.

The discrepancy arises from the different determination of the normal forces N on the joint planes. The author projects the weight vector of the wedge onto a direction normal to the joint planes. In rock mechanics, the component of the weight vector perpendicular to the joint intersection is equilibrated by two forces normal to the joint planes. This procedure implicitly assumes a horizontal force in the wedge parallel to the slope. The method used by the author implicitly assumes no horizontal force. The writer has performed a wedge analysis explicitly considering horizontal forces (14) and concludes that they are important.

Appendix.—References

15. Hendron, A. J. Jr., Cording, E. J., Aiyer, A. K., "Analytical and Graphical Methods for the Analysis of Slopes in Rock Masses," Technical Report No. 36 by University of Illinois to Nuclear Cratering Group, U.S. Army Corps of Engineers, 1971.
16. Hoek, E. and Bray, J. W., "Rock Slope Engineering," Institution of Mining and Metallurgy, London, 1974.

Air Diffusion through Membranes in Triaxial Tests[a]

Discussion by Hermann Winter[4] and Michael Goldscheider[5]

The authors of the paper dealt with the problem of air diffusion through membranes. It is well known that the exact measurement of the pore pressure

[a] October, 1977, by Wayne S. Pollard, Dwight A. Sangrey, and Steve J. Poulos (Proc. Paper 13250).

[4] Research Asst., Inst. for Soil and Rock Mechanics, Univ. of Karlsruhe, Karlsruhe, West Germany.

[5] Sr. Research Asst., Inst. for Soil and Rock Mechanics, Univ. of Karlsruhe, Karlsruhe, West Germany.